PHYSICAL SCIENCES

Explaining recurring maser flares in the ISM through large-scale entangled quantum mechanical states

Fereshteh Rajabi[1] and Martin Houde[1,2]*

We apply Dicke's theory of superradiance (introduced in 1954) to the 6.7-GHz methanol and 22-GHz water spectral lines, often detected in molecular clouds as signposts for the early stages of the star formation process. We suggest that superradiance, characterized by burst-like features taking place over a wide range of time scales, may provide a natural explanation for the recent observations of periodic and seemingly alternating methanol and water maser flares in G107.298+5.639. Although these observations would be very difficult to explain within the context of maser theory, we show that these flares may result from simultaneously initiated 6.7-GHz methanol and 22-GHz water superradiant bursts operating on different time scales, thus providing a natural mechanism for their observed durations and time ordering. The evidence of superradiance in this source further suggests the existence of entangled quantum mechanical states, involving a very large number of molecules, over distances of up to a few kilometers in the interstellar medium.

INTRODUCTION

Since their first detection in the OH 18-cm lines (*1*), a large number of masers from several molecules were discovered in both galactic and extragalactic environments. The main characteristics of masers include high brightness temperatures, corresponding to very high emission intensities over small spatial scales, narrow linewidths, and occasionally high levels of polarization across the spectral lines (*2*, *3*). These attributes of the maser action result from the stimulated emission process in a medium where a population inversion is established and maintained, leading to large amplifications along optical paths exhibiting good velocity coherence for the spectral line under consideration.

In addition, observations show that some maser sources exhibit significant intensity variability on time scales ranging from days to several years. For example, the 22-GHz water masers in Orion-KL (Kleinmann-Low) exhibited drastic flux density variations over a 6-year period between 1979 and 1985 (*4*, *5*). This phase of activity was followed by a 12-year quiescent period that ended in 1997, when subsequent burst activity was detected in this source (*6*). Although most of the flaring sources display abrupt changes in flux density through isolated impulsive phases (*7*), intensity variations in some sources are sometimes found to be periodic, where the corresponding maser transition regularly alternates between phases of high activity and quiescence (*8*, *9*). Although a number of models are proposed to explain these time variations, the underlying mechanism for most of these observations still remains obscure (*9*, *10*).

Some of the aforementioned requirements for the maser action, that is, population inversion and velocity coherence, are also necessary for superradiance; a fundamentally different radiation enhancement process. Superradiance, introduced by Dicke in 1954, is a coherent and cooperative quantum mechanical phenomenon by which a group of N-inverted atoms or molecules emit a radiation pulse (burst) of intensity proportional to N^2. Although virtually unknown to astrophysicists, superradiance has become a very intense research field within the physics community since its introduction by Dicke (*11*, *12*) and its initial laboratory confirmation by Skribanowitz *et al.* (*13*) [see also (*14*, *15*)]. Because superradiant pulses can exhibit a temporal behavior resembling that of flares discovered for some masers in the circumstellar envelope of evolved stars or elsewhere in the interstellar medium (ISM), we recently started investigating the possibility of superradiance within the context of astrophysics. We concluded that it could, in principle, take place in some regions when the necessary conditions are met [that is, population inversion, velocity coherence, and long dephasing time scales compared with those characterizing superradiance (*16*, *17*)].

Here, we extend our analysis to the 6.7-GHz methanol and 22-GHz water maser transitions using the one-dimensional superradiance formalism presented by Rajabi and Houde (*16*, *17*). We start with a brief summary of the important parameters used in our numerical analyses of recent observations of periodic and seemingly alternating flares of 6.7-GHz methanol and 22-GHz water masers in the G107.298+5.639 star-forming region. We end with a brief conclusion, whereas further observational evidence for superradiance in star-forming regions for the methanol (in G33.64–0.21) and water (in Cepheus A) lines is provided in the Supplementary Materials.

SUPERRADIANCE MODEL

As was recently discussed by Rajabi and Houde (*16*, *17*), a rapid and significant increase (sometimes followed by oscillations) in radiation intensity is a behavior typical of a (large-sample) superradiant system. In particular, the analyses of Rajabi and Houde (*16*) established that superradiance may provide a viable explanation for the observed OH 1612-MHz intensity bursts detected in the Mira star U Orionis (*18*) and the preplanetary nebula IRAS 18276-1431 (*19*). The response of a superradiant system is characterized by a few parameters, the most important being the characteristic time scale of superradiance T_R, which is given by

$$T_R = \tau_{sp}\frac{8\pi}{3nL\lambda^2} \quad (1)$$

where τ_{sp} is the spontaneous decay time scale of a single molecule (that is, the inverse of the Einstein spontaneous emission coefficient), n is the density of inverted molecules taking part in the superradiant process, L is the length of the (cylindrical) large sample (thus, nL is the column density of inverted molecules), and λ is the wavelength of the radiation interacting with the molecules in the superradiance system. For a given transition, λ and τ_{sp} are fixed, and T_R thus only depends on the column density of molecules partaking in superradiance.

[1]Department of Physics and Astronomy, University of Western Ontario, London, Ontario, Canada. [2]Division of Physics, Mathematics, and Astronomy, California Institute of Technology, Pasadena, CA 91125, USA.
*Corresponding author. Email: mhoude2@uwo.ca

When a superradiant system is inverted through some pumping mechanism and a critical threshold for the inverted column density is met or exceeded (see Eq. 3 below), the energy stored in the system is released after the so-called delay time τ_D given by

$$\tau_D \simeq \frac{T_R}{4}\left|\ln\left(\frac{\theta_0}{2\pi}\right)\right|^2 \quad (2)$$

with the initial Bloch angle $\theta_0 = 2/\sqrt{N}$, where N is the number of inverted molecules in the sample (*14*, *15*). Whereas the delay time τ_D gives an estimate of the time when the first superradiance burst takes place, the characteristic time T_R sets the duration of each burst. In a superradiance large sample, the energy can be radiated away in a series of bursts, through a phenomenon known as the ringing effect. The number of ringing oscillations varies as a function of T', the time scale of the most important dephasing effect (for example, collisions) that will tend to work against the superradiance phenomenon.

In a more general sense, superradiance can only be observed if $\tau_D < T'$ [see (*16*, *17*) for more details], and this implies the existence of the aforementioned threshold in inverted-population column density

$$(nL)_{crit} \approx \frac{2\pi}{3\lambda^2}\frac{\tau_{sp}}{T'}\left|\ln\left(\frac{\theta_0}{2\pi}\right)\right|^2 \quad (3)$$

which must be met for the initiation of superradiance. More precisely, for column densities below this critical value, the dephasing effects prevent coherent interactions and the system operates in a maser regime. As soon as $nL \geq (nL)_{crit}$, the system switches to a superradiance mode and the masing region breaks into a large number of superradiance large samples for which this condition is met (*16*). Whether $(nL)_{crit}$ is crossed through a slow increase in pumping of the inverted column density or a fast population-inverting pulse is irrelevant. It only matters that the condition $nL \geq (nL)_{crit}$ is somehow reached.

To test our superradiance model, we have chosen T_R and T' as free parameters in the fitting process to intensity curves given by the data presented below. However, note that, as was observed by Rajabi and Houde (*16*) for the OH 1612-MHz line superradiance bursts in U Orionis and IRAS 18276-1431, the volume occupied by a single superradiant large sample is several orders of magnitude smaller than a typical maser region. A similar statement applies to the cases studied in this paper. It follows that the superradiance intensity curves must result from the contributions of a very large number of separate, but approximately simultaneously triggered, superradiant samples. To account for this, we have therefore augmented our one-dimensional superradiance model (*16*) by averaging over several realizations of superradiance samples for which a common T' is used. These realizations result from a Gaussian-distributed ensemble of T_R values of mean $\langle T_R \rangle$ and SD σ_{T_R}.

6.7-GHz METHANOL AND 22-GHz WATER FLARES IN G107.298+5.639

G107.298+5.639 is an intermediate-mass young stellar object deeply embedded in the molecular cloud L1204/S140 (*20*) at a distance of ~0.9 kpc (*21*). For the period July to December 2014 and similarly in 2015, Szymczak *et al.* (*20*) monitored 6.7-GHz methanol and 22-GHz water masers in this source with the Torun 32-m Radio Telescope. During high-activity intervals, the methanol observation rate was increased to eight times a day, whereas in quiescent periods, they were conducted only once a week. However, the water observations were repeated daily with eight gaps of 4 to 5 days of no observations.

The observations of the 6.7-GHz methanol masers indicated four spectral features, among which the $v_{lsr} = -7.4$ km s^{-1}, -8.6 km s^{-1}, and -9.2 km s^{-1} components exhibited a 34.4-day cyclic behavior. Faint cyclic emission was also detected in a few other features in the velocity ranging from $v_{lsr} = -17.2$ km s^{-1} to -13.6 km s^{-1}, although these components were not visible in all cycles. The methanol components showed strong flux variations in the form of repeating (lone) bursts lasting for 4 to 12 days.

The 22-GHz water maser emission was also detected in six spectral features at velocities ranging from $v_{lsr} = -18.3$ km s^{-1} to -1.1 km s^{-1}. Some features (for example, those near $v_{lsr} = -16.5$ km s^{-1} and -8 km s^{-1}) peaked in intensity with the same periodicity as, but delayed relative to, methanol flares at velocities located within ± 1.1 km s^{-1} of those of the water masers themselves. A similar behavior was detected at a velocity near $v_{lsr} = -11.0$ km s^{-1}, where methanol and water flares were also observed in alternation. On the basis of high-angular resolution data sets collected by the European VLBI (Very Long Baseline Interferometry) Network and VLBI Exploration of Radio Astrometry (*22*), Szymczak *et al.* (*20*) concluded that some of the periodically alternating methanol and water flares originate from the same molecular gas volume size of 30 to 80 AU (astronomical units).

To find a viable explanation for these observations, a number of scenarios were examined, but none could adequately reproduce the observations. The alternation of the water and methanol maser bursts is the main feature to be explained. However, this is very difficult to achieve within the context of maser theory, even with the assumptions that the two types of masers happen in the same region and are being periodically enhanced by some pulsating pumping source. For example, it is hard to conceive how the water and methanol maser features would then occur in alternation while also showing different time durations for their flares. We now show how this kind of behavior could naturally arise and may be expected, when studied within the context of Dicke's superradiance.

We assume that we are in the presence of a periodically changing pumping source that simultaneously acts on the population levels of both the 22-GHz water and 6.7-GHz methanol transitions. Although we are not aware of any other observations (aside from the periodic maser flares discussed here) that could provide evidence for this scenario in G107.298+5.639, we know of at least one other young protostellar system where strong, cyclic variations in infrared luminosity have been observed with a period comparable to that seen in G107.298+5.639 [that is, 25.34 days for LRLL 54361 (*23*)]. These infrared intensity variations could, in principle, directly affect the pumping level of maser transitions.

Note that for a given inverted column density, the value of T_R, and therefore the duration of superradiant bursts for a spectral line, scales as τ_{sp}/λ^2 (see Eq. 1). It follows that under similar conditions (that is, assuming for the moment $(nL)_{CH_3OH} \approx (nL)_{H_2O}$), we should expect a superradiance time scale ratio of about 1:8.7 between the 6.7-GHz methanol and 22-GHz water lines, respectively. This expected relationship between T_{R,CH_3OH} and T_{R,H_2O} provides us with the needed element to explain the observations of Szymczak *et al.* (*20*); that is, because T_R sets both the duration of a superradiant burst and the time delay τ_D before its emergence (see Eq. 2), it is to be expected that the methanol flares will be narrower and appear earlier than those of water. Evidently, it is unlikely that the inverted column densities for methanol at 6.7 GHz and water at 22 GHz will be the same, and we thus relax this approximation in what follows. However, the above scenario should still hold for cases where their difference is not too pronounced.

Given the observed duration of flares for the 6.7-GHz methanol and 22-GHz water masers, we adjusted the values of T_R for these transitions to reproduce superradiant bursts of similar time scales (that is, about 10 days for methanol and 30 days for water). The result of our analysis is shown in Fig. 1. The superradiance intensity models (solid curves) were calculated using ensembles of 1000 superradiance large samples (the shape of an intensity curve converges after a few hundred realizations were averaged) tailored to the flaring event occurring between MJD (Modified Julian Day) 57,260 to 57,300 in Fig. 3 of Szymczak *et al.* (*20*) (that is, day 7260 to 7300 in our Fig. 1) for the $v_{lsr} = -8.57$ km s^{-1} 6.7-GHz methanol (red dots) and $v_{lsr} = -7.86$ km s^{-1} 22-GHz water (blue dots) spectral features. As mentioned earlier, these flares were repeated on an approximately 34.4-day period (*20*). For methanol, the model parameters are $\langle T_R\rangle_{CH_3OH} = 2.1$ hours, $\sigma_{T_{R,CH_3OH}} = 0.07\langle T_R\rangle_{CH_3OH}$, and $T'_{CH_3OH} = 90\langle T_R\rangle_{CH_3OH}$, yielding a mean inverted column density of $\langle nL\rangle_{CH_3OH} \approx 3.5 \times 10^4$ cm^{-2}, whereas for water, the parameters are $\langle T_R\rangle_{H_2O} = 7.7$ hours, $\sigma_{T_{R,H_2O}} = 0.04\langle T_R\rangle_{H_2O}$, $T'_{H_2O} = 70\langle T_R\rangle_{H_2O}$, and $\langle nL\rangle_{H_2O} \approx 8.4\times 10^4$ cm^{-2}. In both cases, the models were scaled in intensity to the data. As seen in the figure, the methanol superradiance curve provides a very good fit to the corresponding data, especially in the wings, whereas the water superradiance intensity curve captures well the overall behavior of the water flare, although there is a fair amount of scatter in the data. Note that, despite the apparent time-ordering in the emergence of the methanol and water flares, both superradiance models were initiated at the same time, on day 7261.5. The alternation between the methanol and water bursts observed in Fig. 3 of Szymczak *et al.* (*20*) may thus be readily, and simply, explained by the fact that $\langle T_R\rangle_{H_2O} \approx 3.7\langle T_R\rangle_{CH_3OH}$, which would delay the appearance of the water flare (from Eq. 2) and broaden it relative to methanol. We note that strict simultaneity in the excitation of the two species is not an absolute requirement for superradiance to fit the data, but it is telling that it can provide a viable model even if simultaneity is realized. Although one could conceive models based on maser theory alone to account for the different time scales between the water and methanol intensity bursts (for example, by invoking nonradiative excitation processes, such as grain mantle evaporation or dust heating, followed by reemission), our model has the advantage of being simpler because it is solely based on the difference between the characteristic time scales $\langle T_R\rangle_{H_2O}$ and $\langle T_R\rangle_{CH_3OH}$. The two inverted-population column densities have comparable means (that is, $\langle nL\rangle_{H_2O} \approx 2.4\langle nL\rangle_{CH_3OH}$) and correspond to large-sample lengths of $\langle L\rangle_{CH_3OH} \approx 3.5 \times 10^5$ cm and $\langle L\rangle_{H_2O} \approx 8.4 \times 10^4$ cm when $\langle n\rangle_{CH_3OH} = 0.1$ cm^{-3} and $\langle n\rangle_{H_2O} = 1$ cm^{-3}. As stated earlier, these length scales are markedly smaller than those typical of masers, implying the presence of a large number of superradiance samples.

Finally, it remains to be explained how the broader water intensity flares stay synchronized to the overall 34.4-day period between successive events, as shown in Fig. 3 of Szymczak *et al.* (*20*); that is, the methanol bursts are short and end well before the appearance of the subsequent flaring event, but our water superradiance model in Fig. 1 seems to indicate that the tail of the corresponding curve extends beyond the start of the next eruption cycle. The observed synchronization probably results from the fact that the arrival of the new pumping event responsible for the next flares resets the large samples by reestablishing the inverted populations, which, in effect, terminates the water superradiance cascade and associated flare (that is, truncates our superradiance model curve). The intensity then tends to go to zero but superradiance is once more triggered, resulting in the appearance of the next burst in intensity. This regenerative pumping phenomenon has previously been observed in laboratory superradiance experiments (*24*, *25*).

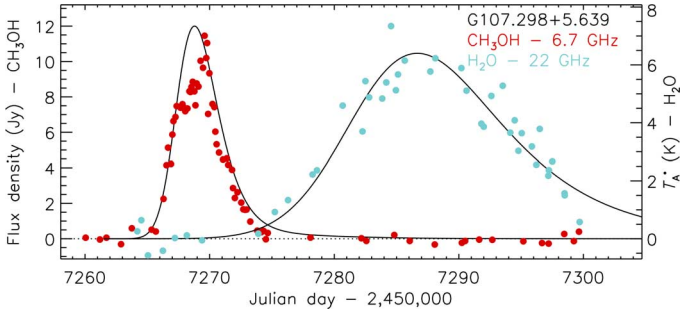

Fig. 1. Superradiance models (solid curves) for the G107.298+5.639 flaring event occurring between MJD 57,260 to 57,300 in Fig. 3 of Szymczak *et al.* (*20*) (that is, day 7260 to 7300 in our figure) for the $v_{lsr} = -8.57$ km s^{-1} 6.7-GHz methanol (red dots) and $v_{lsr} = -7.86$ km s^{-1} 22-GHz water (blue dots) spectral features. These flares were repeated on an approximately 34.4-day period (*20*). The methanol and water data/models use the vertical axes on the left-hand and right-hand sides, respectively. For methanol, the model parameters are $\langle T_R\rangle_{CH_3OH} = 2.1$ hours, $\sigma_{T_{R,CH_3OH}} = 0.07\langle T_R\rangle_{CH_3OH}$, and $T'_{CH_3OH} = 90\langle T_R\rangle_{CH_3OH}$, yielding a mean inverted column density of $\langle nL\rangle_{CH_3OH} \approx 3.5 \times 10^4$ cm^{-2}, whereas for water, the parameters are $\langle T_R\rangle_{H_2O} = 7.7$ hours, $\sigma_{T_{R,H_2O}} = 0.04\langle T_R\rangle_{H_2O}$ $T'_{H_2O} = 70\langle T_R\rangle_{H_2O}$, and $\langle nL\rangle_{H_2O} \approx 8.4 \times 10^4$ cm^{-2}. Both superradiance models were initiated at the same time, on day 7261.5. Data is taken from Szymczak *et al.* 2016 (*20*). See Supplementary Materials for data.

CONCLUSION

When combined with the recently reported evidence for this phenomenon in the environments of evolved stars (*16*), the discovery of superradiance in star-forming regions would broaden the applicability of our model and further establish the existence of a previously unsuspected physical phenomenon in the ISM. The occurrence of superradiance in astrophysical objects would also imply the presence of entangled quantum mechanical systems, involving a very large number of molecules, over distances of up to a few kilometers in the ISM, which can also be of interest for quantum information research.

MATERIALS AND METHODS

The data of 22-GHz water and 6.7-GHz methanol in G107.298+5.639 discussed in the main part of the paper were published by Szymczak *et al.* (*20*) and provided for our analysis by the authors. The data of 6.7-GHz methanol in G33.64-0.21 presented in the Supplementary Materials were previously published by Fujisawa *et al.* (*27*) and provided to us by the authors, whereas the 22-GHz water observations in Cepheus A were taken from Mattila *et al.* (*7*). All these data sets were analyzed by numerically solving the one-dimensional sine-Gordon equation (*14*–*17*). As stated earlier, we augmented this model by averaging over several realizations of cylindrical superradiance samples taken from a Gaussian-distributed ensemble of T_R values of mean $\langle T_R\rangle$ and SD σ_{T_R}.

To minimize diffraction and transverse effects not included in our one-dimensional model, we set the dimensions of the superradiance samples by imposing a Fresnel number of unity (*14*). This also ensured that the size of the samples did not exceed the condition necessary for phase coherence to be maintained across their length [that is, $L \sim \lambda/\phi_B$, where λ is the wavelength and ϕ_B is the beam solid angle of the radiation; for example, see (*3*)].

SUPPLEMENTARY MATERIALS

Supplementary material for this article is available at http://advances.sciencemag.org/cgi/content/full/3/3/e1601858/DC1

Supplementary Text
fig. S1. A superradiance large-sample intensity model (solid blue curve) superposed on the data from Fujisawa *et al.* (*27*) (black dots) obtained in July and August 2009 for the second 6.7-GHz methanol burst in G33.64-0.21.
The data presented in fig. S1 (black dots) from Fujisawa *et al.* (*27*) obtained in July and August 2009 for the second 6.7-GHz methanol burst in G33.64-0.21.
fig. S2. A superradiance large-sample intensity model (solid blue curve) superposed on the data from Mattila *et al.* (*7*) (black dots) obtained in April and May 1983 for the 22-GHz water burst at $v_{lsr} = -11.2$ km s^{-1} in Cepheus A.
The data presented in fig. S2 (black dots) from Mattila *et al.* (*7*) obtained in April and May 1983 for the 22-GHz water burst at $v_{lsr} = -11.2$ km s^{-1} in Cepheus A.
The data presented in Fig. 1 for the G107.298+5.639, illustrating the burst for the $v_{lsr} = 8.57$ km s^{-1} 6.7-GHz methanol (red dots) between MJD 57,260 and 57,300 taken from Szymczak *et al.* 2016 (*20*).
The data presented in Fig. 1 for the G107.298+5.639, illustrating the burst for $v_{lsr} = 7.86$ km s^{-1} 22-GHz water (blue dots in the figure).
References (*26*–*29*)

REFERENCES AND NOTES

1. H. Weaver, D. R. W. Williams, N. H. Dieter, W. T. Lum, Observations of a strong unidentified microwave line and of emission from the OH molecule. *Nature* **208**, 29–31 (1965).
2. M. Gray, in *Maser Sources in Astrophysics* (Cambridge, 2012).
3. M. Elitzur, in *Astronomical Masers* (Kluwer, 1992).
4. G. Garay, J. M. Moran, A. D. Haschick, The Orion-KL super water maser. *Astrophys. J.* **338**, 244–261 (1989).
5. L. I. Matveenko, D. A. Graham, P. J. Diamond, The H_2O maser flare region in the Orion-KL nebula. *Astron. Lett.* **14**, 468–476 (1988).
6. T. Omodaka, T. Maeda, M. Miyoshi, A. Okudaira, M. Nishio, T. Miyaji, N. Motiduki, M. Morimoto, H. Kobayashi, T. Sasao, The enormous outburst of the 7.9 km s^{-1} water-maser feature in Orion KL. *Publ. Astron. Soc. Jpn.* **51**, 333–336 (1999).
7. K. Mattila, N. Holsti, M. Toriseva, R. Anttila, L. Malkamaki, Rapid outbursts in the water maser Cepheus A. *Astron. Astrophys.* **145**, 192–200 (1985).
8. M. Szymczak, P. Wolak, A. Bartkiewicz, Discovery of four periodic methanol masers and updated light curve for a further one. *Mon. Not. R. Astron. Soc.* **448**, 2284–2293 (2015).
9. S. Goedhart, M. J. Gaylard, D. J. van der Walt, Periodic flares in the methanol maser source G9.62+0.20E. *Mon. Not. R. Astron. Soc.* **339**, L33–L36 (2003).
10. S. Y. Parfenov, A. M. Sobolev, On the Class II methanol maser periodic variability due to the rotating spiral shocks in the gaps of discs around young binary stars. *Mon. Not. R. Astron. Soc.* **444**, 620–628 (2014).
11. R. H. Dicke, Coherence in spontaneous radiation processes. *Phys. Rev.* **93**, 99–110 (1954).
12. R. H. Dicke, The coherence brightened laser. *Quantum Electron.* **1**, 35–54 (1964).
13. N. Skribanowitz, I. P. Herman, J. C. MacGillivray, M. S. Feld, Observation of Dicke superradiance in optically pumped HF gas. *Phys. Rev. Lett.* **30**, 309–312 (1973).
14. M. Gross, S. Haroche, Superradiance: An essay on the theory of collective spontaneous emission. *Phys. Rep.* **93**, 301–396 (1982).
15. M. G. Benedict, A. M. Ermolaev, V. A. Malyshev, I. V. Sokolov, E. D. Trifonov, in *Super-radiance: Multiatomic Coherent Emission* (IOP, 1996).
16. F. Rajabi, M. Houde, Dicke's superradiance in astrophysics. II – The OH 1612 MHz line. *Astrophys. J.* **828**, 57–67 (2016).
17. F. Rajabi, M. Houde, Dicke's superradiance in astrophysics. I – The 21 cm line. *Astrophys. J.* **826**, 216–231 (2016).
18. P. R. Jewell, J. C. Webber, L. E. Snyder, Evolution of the OH maser emission from U Orionis. *Astrophys. J.* **249**, 118–123 (1981).
19. P. Wolak, M. Szymczak, A. Bartkiewicz, E. Gerard, Violent maser events in the cirumstellar envelope of the pre-planetary nebula IRAS18276-1431. *Proceedings of the 12th European VLBI Network Symposium and Users Meeting (EVN 2014)* 116–119 (2014).
20. M. Szymczak, M. Olech, P. Wolak, A. Bartkiewicz, M. Gawrónski, Discovery of periodic and alternating flares of the methanol and water masers in G107.298+5.639. *Mon. Not. R. Astron. Soc.* **459**, L56–L60 (2016).
21. D. Crampton, W. A. Fisher, Spectroscopic observations of stars in H II regions. *Publ. Dom. Astrophys. Obs., Victoria* **14**, 283–304 (1974).
22. T. Hirota, K. Ando, T. Bushimata, Y. K. Choi, M. Honma, H. Imai, K. Iwadate, T. Jike, S. Kameno, O. Kameya, R. Kamohara, Y. Kan-ya, N. Kawaguchi, M. Kijima, M. K. Kim, H. Kobayashi, S. Kuji, T. Kurayama, S. Manabe, M. Matsui, N. Matsumoto, T. Miyaji, A. Miyazaki, T. Nagayama, A. Nakagawa, D. Namikawa, D. Nyu, C. S. Oh, T. Omodaka, T. Oyama, S. Sakai, T. Sasao, K. Sato, M. Sato, K. M. Shibata, Y. Tamura, K. Ueda, K. Yamashita, Astrometry of H_2O masers in nearby star-forming regions with VERA III. IRAS 22198+6336 in Lynds1204G. *Publ. Astron. Soc. Jpn.* **60**, 961–974 (2008).
23. J. Muzerolle, E. Furlan, K. Flaherty, Z. Balog, R. Gutermuth, Pulsed accretion in a variable protostar. *Nature* **493**, 378–380 (2013).
24. E. Paradis, B. Barrett, A. Kumarakrishnan, R. Zhang, G. Raithel, Observation of superfluorescent emissions from laser-cooled atoms. *Phys. Rev. A* **77**, 043419 (2008).
25. M. Gross, C. Fabre, P. Pillet, S. Haroche, Observation of near-infrared Dicke superradiance on cascading transitions in atomic sodium. *Phys. Rev. Lett.* **36**, 1035–1038 (1976).
26. K. Fujisawa, G. Takase, S. Kimura, N. Aoki, Y. Nagadomi, T. Shimomura, K. Sugiyama, K. Motogi, K. Niinuma, T. Hirota, Y. Yonekura, Periodic flare of the 6.7-GHz methanol maser in IRAS 22198+6336. *Publ. Astron. Soc. Jpn.* **66**, 78–85 (2014).
27. K. Fujisawa, K. Sugiyama, N. Aoki, T. Hirota, N. Mochizuki, A. Doi, M. Honma, H. Kobayashi, N. Kawaguchi, H. Ogawa, T. Omodaka, Y. Yonekura, Bursting activity in a high-mass star-forming region G33.64-0.21 observed with the 6.7 GHz methanol maser. *Publ. Astron. Soc. Jpn.* **64**, 17 (2012).
28. D. M. Cragg, A. M. Sobolev, P. D. Godfrey, Models of Class II methanol masers based on improved molecular data. *Mon. Not. R. Astron. Soc.* **360**, 533–545 (2005).
29. M. Elitzur, D. J. Hollenbach, C. F. McKee, H_2O masers in star-forming regions. *Astrophys. J.* **346**, 983–990 (1989).

Acknowledgments: We thank M. Szymczak for sharing her data of G107.298+5.639. We would also like to thank K. Fujisawa for making his data of G33.64-0.21 available to us, provided in the Supplementary Materials. We are grateful to S. Metchev and J. Cami for their useful suggestions and comments. **Funding:** M.H.'s research is funded through the Natural Sciences and Engineering Research Council of Canada Discovery Grant RGPIN-2016-04460 and the Western Strategic Support for Research Accelerator Success. **Author contributions:** Both authors contributed to the science discussion and to the writing of the paper. F.R. obtained and analyzed the data, and M.H. produced the figures appearing in the paper. **Competing interests:** The authors declare that they have no competing interests. **Data and materials availability:** All data needed to evaluate the conclusions in the paper are present in the paper and/or the Supplementary Materials. Additional data related to this paper may be requested from the authors.

Submitted 9 August 2016
Accepted 9 February 2017
Published 24 March 2017
10.1126/sciadv.1601858

Citation: F. Rajabi, M. Houde, Explaining recurring maser flares in the ISM through large-scale entangled quantum mechanical states. *Sci. Adv.* **3**, e1601858 (2017).

Explaining recurring maser flares in the ISM through large-scale entangled quantum mechanical states

Fereshteh Rajabi and Martin Houde

Sci Adv **3** (3), e1601858.
DOI: 10.1126/sciadv.1601858